Marine and Petroleum Geology 88 (2017) 551–554

Contents lists available at ScienceDirect

Marine and Petroleum Geology

journal homepage: www.elsevier.com/locate/marpetgeo

Brittle rotational faults and the associated shear heating

Soumyajit Mukherjee [a,*], M.M. Khonsari [b]

[a] Department of Earth Sciences, Indian Institute of Technology Bombay, Powai, Mumbai 400 076, Maharashtra, India
[b] Department of Mechanical and Industrial Engineering, Louisiana State University, Baton Rouge, LA 70803, USA

ARTICLE INFO

Article history:
Received 3 June 2017
Received in revised form
1 September 2017
Accepted 4 September 2017
Available online 7 September 2017

Keywords:
Brittle shear
Frictional heating
Rotational fault
Structural geology
Tribology

ABSTRACT

Brittle faulting-related shear heating is important in petroleum geosciences, tectonics and seismic studies. Temporal variation of shear heat related temperature rise for rotational and roto-translational faults are investigated in this work. For planar fault planes, devoid of gouge and any secondary faulting, temperature rise is proportional to the coefficient of friction, and rate of (angular) slip. Tectonically realistic physical parameters for rotational faults, especially prolonged faulting, can significantly increase temperature by shear heating at shallow crustal depth, capable of thermal maturity of hydrocarbons.

1. Introduction

Brittle fault planes are discussed ideally, under the general category of “non-rotational faults” or “translational faults”, as having equal magnitude of net slip at every point along the fault trend (Neuendorf et al., 2005). On the other hand, much less discussed, yet widely recognized (e.g., Behr et al., 2010), are the second category of rotational faults where the fault blocks rotate with respect to one another. The sense of rotation is described as clockwise or anti-clockwise, based on the sense of rotation of the rear faulted block (Ekins, 1987). The ‘scissor axis’ (Keary, 1993)/axis of rotation remains orthogonal to the fault plane. “Rotational faults” (rarely called “point faults”: Qazi, 2004) have been described by a number of other terms (Fig. 1a–c and captions). These faults can have planar or curvi-planar surfaces (referred in Ghosh, 1993; Marshak and Mitra, 1988), numerous in some particular terrains (Nevin, 1949), and have temporally shifting pivot of rotation (Billings, 1972). Translational faults, identified based on limited observations, can actually have rotational components (Ekins, 1987; Martel, 1999; van der Pluijm and Marshak, 2004). Bookshelf gliding too sometimes is considered as a rotational fault (Wernicke and Burchfiel, 1982), where in addition to the faulted blocks, the fault planes themselves rotate.

Rotational fault planes can run as long as 8 km (ref: Wisconsin Utilities Project) with ~76 m of vertical throw (Warner, 2000). As no reports of circular slickensides exposed on fault planes exists in the geological literature, it seems neither a perfect hinge-/scissors (Fig. 1b1) nor a pivotal fault ((Fig. 1b2) exists in nature. Instead, curved slickensides remarkably different than circular arcs (e.g., Otsubo et al., 2013 as prototype; Mandal and Chakraborty, 1989 in analytical models) indicate that most of them are roto-translational (Fig. 1c).

Shear heating/frictional heating is an important aspect of studying brittle (and also ductile: Mukherjee and Mulchrone, 2013; Mulchrone and Mukherjee 2015, 2016) faults. Several theoretical works on such heating has been published for translational faults (Cardwell et al., 1978; Mukherjee, 2017). In general, friction-related temperature of the reverse faulted blocks is proportional to the coefficient of friction, and the thickness of the hangingwall block (Mukherjee, 2017). In particular, heat budget has been worked out in detail for the San Andreas Fault (Chester et al., 1993). To gain insight, this article develops simple models of shear heating for the rotational faults —an interdisciplinary aspect at the interface of structural geology and tribology. Kinematics of rotational faults is already discussed in Mandal and Chakraborty (1989). Seismicity, landslides (Geist, 2000), contact metamorphism (Sasada, 1979) and thermal maturity of hydrocarbons (Keym et al., 2006) can also be induced by/related with rotational faults. Therefore, modeling shear heating for such faults can explain better those natural phenomena.

* Corresponding author.
E-mail address: soumyajitm@gmail.com (S. Mukherjee).

http://dx.doi.org/10.1016/j.marpetgeo.2017.09.003
0264-8172/

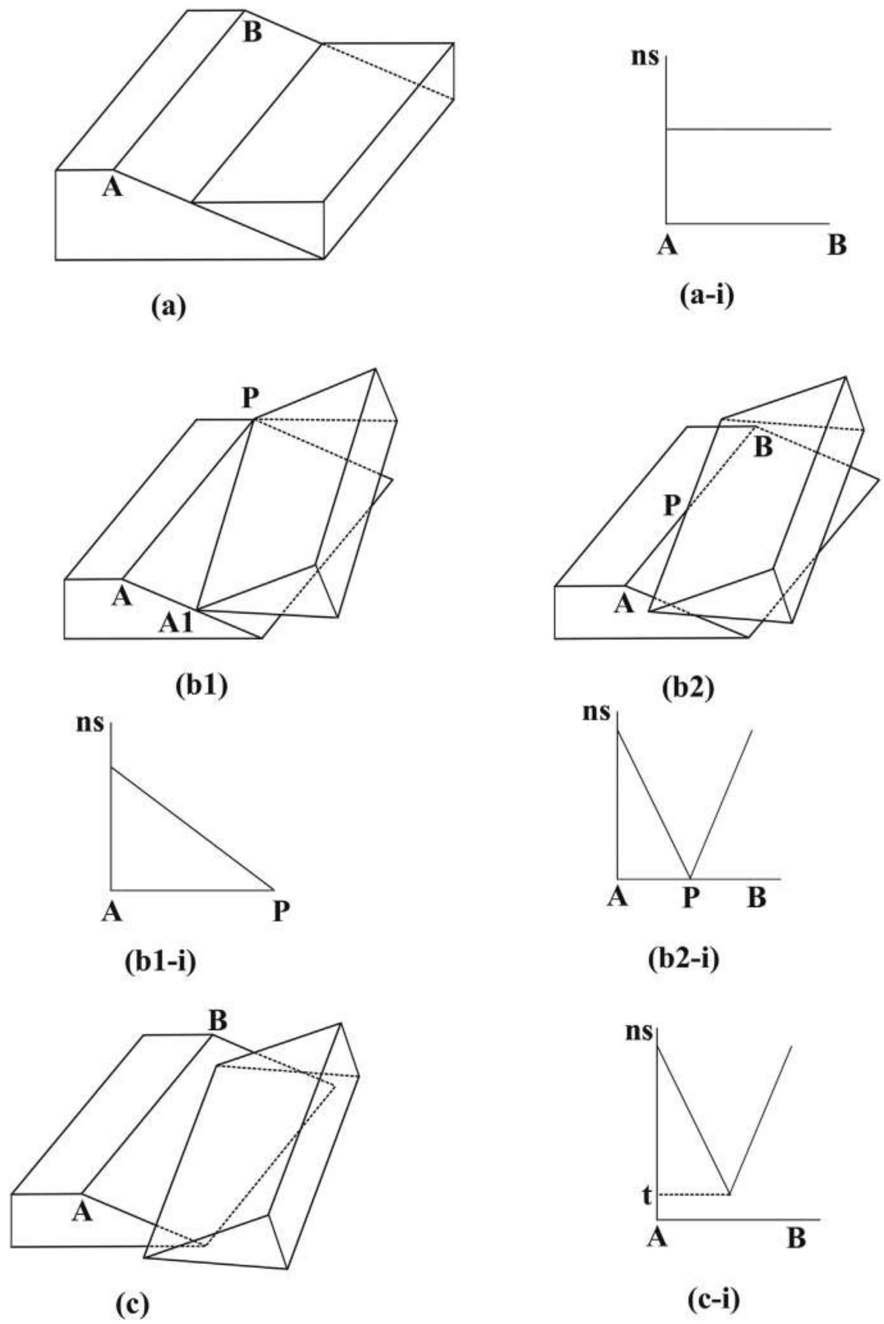

Fig. 1. a. Translational dip slip normal fault. b. Rotational faults with clockwise rotation sense: b1: hinge fault as per Donath (1962) but scissor fault as per Roberts (1982); b2: pivotal fault as per Donath (1962); c: roto-translational fault. Point P: 'center of rotation' (as per Donath, 1962) or pivot; t: translational component of net slip. Nomenclature for fault in Fig. 1c is uniquely as per Mandal and Chakraborty (1989), but such as fault has also been called simply a rotational fault by Roberts (1982). Eqn (13) represents its shear heat equation. Eqns (4) and (11) represent those for Figs. 1a and 1b, respectively. a-i, b1-i, b2-i, and c–i: Net slip ('ns') profiles. Referring to Fig. b1, If $\angle$ APA1 = θ in degree unit, and AP length = R, then the net slip along circular arc, through any point A, is = π R θ/180°. Therefore all the linear profiles of net slip in Figs. b1, b2 and c make an acute angle of $\tan^{-1}$ (πθ/180°) with the AB-axis. We define *effective slip* ('es') as the linear distance between the points A and A1.es = 1.41*R{1+cosθ}$^{0.5}$. Obviously es > ns except at pivot (R = 0 case) where es = ns = 0.

2. Model

Consider a dip slip normal translational fault (Fig. 1a), a rotational faults (Fig. 1b), and a roto-translation fault (Fig. 1c), all having a planar fault plane. In case of Fig. 1a, suppose the hangingwall block has mass 'm', the coefficient of friction between the hanging wall and the footwall block be 'μ', the acceleration due to gravity be 'g', the constant linear slip rate be 'V', the time duration of slip be 't', the dip of the fault plane be 'θ', temperature rise by shear heating be ΔT, the 'normal load' exerted by the hangingwall block on the fault plane: N = mgcosθ, and the specific heat of the rock be 'C_p''.

$$\text{Power, } \mathbf{P} = \mu NV \tag{1}$$

$$\text{Or, } \mathbf{P} = \mu mgV\cos\theta \tag{2}$$

We considered work done by fault is entirely converted to heat energy.

$$\text{Shear heat, } Q = mC_p\Delta T = P\Delta t = \mu mg\cos\theta\Delta t \tag{3}$$

Therefore, $\Delta T/\Delta t = \mu g V C_p^{-1} \cos\theta$ (4)

Referring to Fig. 1b1 and 1b2, 'ω' is the angular velocity and '$\overline{W}$' is the uniform load distribution per unit area. Here,

$$dN = \mu \overline{W} dA \tag{5}$$

$$Or,\ N = \overline{W} A \tag{6}$$

Consider a small area 'dA' away from the pivot at a distance 'R' in subsequence lines below.

$$\text{Also, } dP = \mu r \omega dN \tag{7}$$

dP is the power needed to overcome frictional force due to rotational motion of the hangingwall block. Note that constraining the average velocity from the rock record may not always be possible most accurately. One of the reasons for this would be inherent uncertainty in fault gouge dating (e.g., Clauer, 2013). The second possibility would be with rotational faults that are devoid of any gouge material.

$$P = \int_A r\omega dN = \int_A \mu r \omega \overline{W} dA \quad \text{(by substituting dN from eqn 5)} \tag{8}$$

$$P = \mu \omega \overline{W} \int_A r dA = \mu N \omega \left[A^{-1} \int_A r dA \right] \tag{9}$$

Considering the expression inside the brackets on the right-hand-side of eqn (9) as 'average radius for rotation: R_{avg}', we can write,

$$\mathbf{P} = \mu\ mg\ \cos\theta \omega R_{avg} \tag{10}$$

Now, recall eqn (3): Shear heat, $Q = mC_p\Delta T = \mathbf{P}\Delta t$. Using this relation in eqn (10),

$$\Delta T/\Delta t = \mu\ g\ \omega R_{avg} C_p^{-1} \cos\theta \tag{11}$$

Bringing tangential velocity $V_t = \omega R$ in eqn (11),

$$\Delta T/\Delta t = \mu\ g\ V_t C_p^{-1} \cos\theta \tag{12}$$

For the case of Fig. 1c of roto-translational faults, as a simple approximation, the right-hand-side of eqns (4) and (11) may be added up as follows:

$$\Delta T/\Delta t = \mu g C_p^{-1} \cos\theta (V + \omega R_{avg}) \tag{13}$$

3. Discussions & conclusions

This work deduces expressions for shear heat related temporal increase in temperature for rotational- and roto-translational faults. For a scissors/pivotal/hinge fault, temperature rise by shear heating per unit time is proportional to the relative angular velocity between the hangingwall and the footwall block (see eqn. (11)). Obviously, for roto-translational faults when the blocks also have a component of translational veloscity ('V'), this relation does not hold (eqn (13)). As expected, however, in all cases of rotational- and roto-translational faults (Fig. 1b,c), (*i*) temperature rise by shear heating is proportional to the coefficient of friction ('μ'). This matches with the cases of simple translational faults (as in eqns (12) and (13) of Mukherjee, 2017). (*ii*) Temperature rise after instant t is inversely proportional to C_p. This matches with the derivation by Hamada et al. (2009) for a fault zone with translational faulting. Also note that for a horizontal fault plane, i.e., $\theta = 0$, for which $\cos\theta = 1$, shear heat related temperature rise is maximum for all the three cases of translational-, rotational- and roto-translational faults (follow eqns (4), (12) and (13), respectively). On the other hand, as θ increases magnitude, the shear heat related temperature keeps falling, and becomes zero for vertical fault planes ($\theta = 90°$).

Is shear heat related temperature rise in geological cases of rotational faults significant? We do not have all the data necessary to estimate shear heat where rotational faults have been reported, for example that by Behr et al. (2010). Slip rates ('V' in eqns (4) and (12)) for translational faults of various types have been deduced geochronologically, which usually range from a few mm- (Dezes et al., 1999) up to a few cm per year (Kohn et al., 2004). The rotation rate ('ω' in eqns (11) and (12)) in mega-scale can be say $3°\ Ma^{-1}$ (Price and Scott, 1994). Brittle faulting takes place at shallow crustal depth, therefore to estimate shear heat, we need to take C_p at a low temperature. For example, at 20 °C, C_p of gneiss is 770 J kg^{-1} K^{-1} (Waples and Waples, 2004). The average frictional coefficient ('μ') for rocks at geological deformation condition is ~0.3 (Byerlee, 1978). Duration of faulting ('t') can be few seconds, as in case of seiemicity (McGuire and Hanks, 1980), and at least more than a month for aseismic slip (Ohta et al., 2012). On the other hand, slip takes place for tens of thousands of years in collisional tectonic regimes (review in Mukherjee, 2013). Fault dip (θ) can vary widely in deformed terrains from sub-horizontal (in regional thrusting) up to sub-vertical (during isostatic adjustment). However, Keary (1993) referred that rotational faults usually have sub-vertical fault planes. For an estimation of shear heat, we choose the above specified parameters as t = 30 days and $\theta = 86°$. A translational fault active for 30 days, with a slip rate (V) of 2 mm yr^{-1}produces ~ 109 K shear heat (as per eqn (4)). On the other hand, a much faster slip rate of 1 cm $yr^{-1}$for 10^5 yrs produces ~543 K of shear heat (using the same eqn). Now, to compare, for the rotational case, for 2 mm yr^{-1}angular velocity (ω) acting for 10^3 yrs, 937 K of shear heat would be produced (using eqn (12)).

These estimates are approximate since C_p increases with temperature in rocks (Waples and Waples, 2004). As temperature increases with depth, C_p should also increase depth-wise even if we consider a faulted single monomineralic rock unit. Therefore, eqns (4), (12) and (13) work in terrains with a low geothermal gradient.

The presented model considered unfoliated/massive single rock of uniform (thermal-) physical properties that got faulted.

Acknowledgements

A CPDA grant and a research sabbatical for the year 2017 received from IIT Bombay supported SM. Adam Bumby and two anonymous experts are thanked for handling and reviewing the ms, respectively.

References

Behr, W.M., Rood, D.H., Fletcher, K.E., Guzman, N., Finkel, R., Hanks, T.C., Hudnut, K.W., et al., 2010. Uncertainties in slip-rate estimates for the mission creek strand of the southern san Andreas fault at biskra palms Oasis, southern California. Geol. Soc. Am. Bull. 122, 1360–1377.
Billings, M.P., 1972. Structural Geology, third ed. Prentice-Hall of India Pvt. Ltd, p. 178.
Byerlee, J., 1978. Friction of rocks. Pure App. Geophys. 116, 615–626.
Cardwell, R.K., et al., 1978. Frictional heating on a fault zone with finite thickness. Geophys. J. Roy. Astron. Soc. 52, 525–530.
Chester, F.M., Evans, J.P., Beigel, R.L., 1993. Internal structure and weakening mechanisms of the san Andreas Fault. J. Geophys. Res. 98, 771–786.

Clauer, N., 2013. The K-Ar and 40 Ar/39 Ar methods revisited for dating fine-grained K-bearing clay minerals. Chem. Geol. 354, 163–185.
Dezes, P.J., Vannay, J.C., Steck, A., Bussy, F., Cosca, M., 1999. Synorogenic extension: quantitative constraints on the age and displacement of the zanskar shear zone. Geol. Soc. Am. Bull. 111, 364–374.
Donath, F.A., 1962. Analysis of basin-range structure, south-central Oregon. Geol. Soc. Am. Bull. 73, 1–16.
Ekins, P.R., 1987. Faults and faulting. In: Seyfert, C.K. (Ed.), The Encyclopedia of Structural Geology and Plate Tectonics. Van Nostrand Reinhold Co, New York, pp. 228–239.
Geist, E.L., 2000. Origin of the 17 July 1998 Papua New Guinea tsunami: earthquake or landslide. Seismol. Res. Lett. 71, 344–351.
Ghosh, S.K., 1993. Structural Geology: Fundamentals and Modern Developments. Pergamon Press, p. 429.
Hamada, Y., et al., 2009. Estimated dynamic shear stress and frictional heat during the 1999 Taiwan Chi-Chi earthquake: a chemical kinetics approach with isothermal heating experiments. Tectonophysics 469, 73–84.
Keary, P., 1993. The Encyclopedia of the Solid Earth Sciences. John Wiley & Sons, p. 237.
Keym, M., Dieckmann, V., Horsfield, B., Erdmann, M., Galimberti, R., Kua, L.-C., Leith, L., Podlaha, O., 2006. Source rock heterogeneity of the upper jurassic draupne formation, north viking graben, and its relevance to petroleum generation studies. Org. Geochem 37, 220–243.
Kohn, M.J., Wieland, M.S., Parkinson, C.D., Upreti, B.N., 2004. Miocene faulting at plate tectonic velocity in the Himalaya of central Nepal. Earth Planet. Sci. Lett. 228, 299–310.
Mandal, N., Chakraborty, C., 1989. Fault motion and curved slickenlines: a theoretical analysis. J. Struct. Geol. 11, 497–501.
Marshak, S., Mitra, G., 1988. Basic Methods of Structural Geology. Prentice Hall.
Martel, S.J., 1999. Mechanical controls on fault geometry. J. Struct. Geol. 21, 585–596.
McGuire, R.K., Hanks, T.C., 1980. RMS accelerations and spectral amplitudes of strong ground motionduring the San Fernando, California earthquake. Bull. Seismol. Soc. Am. 70, 1907–1919.
Mukherjee, S., 2013. Channel flow extrusion model to constrain dynamic viscosity and Prandtl number of the higher Himalayan Shear Zone. Int. J. Earth Sci. 102, 1811–1835.
Mukherjee, S., 2017. Shear heating by translational brittle reverse faulting along a single, sharp and straight fault plane. J. Earth Sys. Sci. 126 (1).
Mukherjee, S., Mulchrone, K.F., 2013. Viscous dissipation pattern in incompressible Newtonian simple shear zones: an analytical model. Int. J. Earth Sci. 102, 1165–1170.
Mulchrone, K.F., Mukherjee, S., 2015. Shear senses and viscous dissipation of layered ductile simple shear zones. Pure Appl. Geophys. 172, 2635–2642.
Mulchrone, K.F., Mukherjee, S., 2016. Kinematics and shear heat pattern of ductile simple shear zones with 'slip boundary condition'. Int. J. Earth Sci. 105, 1015–1020.
Neuendorf, K.K.E., Mehl Jr., J.P., Jackson, J.A., 2005. Glossary of geology. Am. Geol. Inst. Alex. 162.
Nevin, C.M., 1949. Principles of Structural Geology, p. 88.
Ohta, Y., Hino, R., Inazu, D., Ohzono, M., Ito, Y., Mishina, M., Iinuma, T., Nakajima, J., Osada, Y., Suzuki, K., Fujimoto, H., 2012. Geodetic constraints on afterslip characteristics following the March 9, 2011, Sanriku-oki earthquake, Japan. Geophys. Res. Lett. 39.
Otsubo, M., Shigematsu, N., Imanishi, K., Ando, R., Takahashi, M., Azuma, T., 2013. Temporal slip change based on curved slickenlines on fault scarps along Itozawa fault caused by 2011 Iwaki earthquake, northeast Japan. Tectonophysics 608, 970–979.
Price, S.P., Scott, B., 1994. Fault block rotations at the edge of a zone of continental extension; southwest Turkey. J. Struct. Geol. 16, 381–392.
Qazi, S.A., 2004. Principles of Physical Geography. APH Publishing Corporation, New Delhi, p. 102.
Roberts, J.L., 1982. Introduction to Geological Maps and Structures. Pergamon Press, Oxford, p. 137.
Sasada, M., 1979. Petrological study of the south yubara quartz gabbroic mass, Okyama Prefecture, southwest Japan. J. Jap. Assoc. Mineral. Petrol. Econ. Geol. 74, 1–15.
van der Pluijm, B.A., Marshak, S., 2004. Earth Structure: an Introduction to Structural Geology and Tectonics, second ed., p. 388
Waples, D.W., Waples, J.S., 2004. A review and evaluation of specific heat capacities of rocks, minerals, and subsurface fluids. Part 1: minerals and nonporous rocks. Nat. Resour. Res. 13, 97–121.
Warner, E.M., 2000. Structural Geology and Pressure Compartmentalization of Jonah Field Based on 3-d-seismic Data and Subsurface Geology, Sublette County, Wyoming. The Mountain Geologists.
Wernicke, B., Burchfiel, B.C., 1982. Modes of extensional tectonics. J. Struct. Geol. 4, 105–115.
Wisconsin Utilities Project.Koshkonong nuclear plant units 1 and 2, site addendum, Prelim. Saf. Anal. Rep., Volume 2, Part 2.